Distribution, ecological risk, and source analysis of heavy metals in recent beach sediments of Sharm El-Sheikh, Egypt

Hamdy El Sayed Nour

Abstract To study the distribution of the concentrations and the sources of pollutants and their environmental assessment in the Sharm El-Sheikh coastal area, Fe, Mn, Cu, Zn, Pb, Ni, Cd, and Co concentrations were analyzed in the beach sediments of Sharm El-Sheikh harbor and Sharm El-Maya bay by the atomic absorption spectrophotometer. The results revealed that Sharm El-Sheikh harbor has higher concentrations of Fe, Mn, Ni, and Cd than in Sharm El-Maya bay. Meanwhile, the environmental pollution indicators as enrichment factors, metal pollution index, contamination factors, sediments pollution index, geo-accumulation index, ecological risk factor, and the potential contamination index reported that Sharm El-Sheikh harbor has a higher degree of pollution (MPI = 43.4) than Sharm El-Maya bay (MPI = 38.2). Moreover, both of the studied areas have shown very high contamination of Cd and moderate to high contamination of Pb, Mn, Cu, and Zn. Furthermore, the concentrations of Mn, Cu, Ni, and Cd in the studied area are higher than those in the coasts of Hurghada, Shalateen, Red Sea of Saudi Arabia, and the Russian Caspian Sea. The main sources of the metals in the studied area are the human impacts as tourist activities, boat navigation, large numbers of anchored tourist boats, diving operations, and car fuel combustion products. In addition, the natural weathering of Gabal El-Safra and basement rocks can be counted as natural sources of metals.

Introduction

There are several sources of heavy metals that can enter the environment: firstly, weathering processes of rocks that are rich in different metals in their chemical composition. Secondly, anthropogenic activities such as sewage, shipping, industrial activities, mining, tourist services, painting, renewable boats, and others (Chen et al. 2007; Nour et al. 2018). Marine sediments are a reservoir and a repository of these metals where they are transported directly from the source of pollution or by precipitate from seawater (Selvaraj et al. 2004; Wang 2018).

Sharm El-Sheikh city is one of the most famous tourist cities in Egypt on the Gulf of Aqaba. It is located about 385 km from Suez city (Fig. 1). It is warm in winter and has a hot weather in summer. This city is characterized by a very large number of resorts, hotels, and diving clubs. In view of the significant increase in the rate of development of Sharm El-Sheikh and the continuous increase in hotel and resort construction operations, as well as the increase in the rates of tourism activities, especially diving and boats. This study aims to determine the distribution of toxic heavy metal concentrations in the beach sediments of the most important

H. E. S. Nour (✉)
Geology Department, Faculty of Sciences, Zagazig University, Zagazig, Egypt
e-mail: nour_geo@yahoo.com

sites in the city. Moreover, it aims to assess the potential environmental pollution risk and to identify the potential sources of these pollutants.

To evaluate the status of the environmental risk of the studied area, the metal concentrations were compared with those in other world regions as the Red Sea coast, Mediterranean Sea coast, and the Caspian Sea coast. Moreover, another comparison was made with the background levels, according to the international environmental organizations such as sediment quality guidelines (SQG) (Long et al. 1995), interim sediment quality guideline (ISQG), probable effect level (PEL) (ISQG 1995), background shale (Turekian and Wedepoh 1961), and background continental crust (Taylor 1964).

Material and methods

Study area and sampling

A total of 24 recent beach sediments were collected from Sharm El-Sheikh area at the southern coast of the Sinai Peninsula on the Gulf of Aqaba (Fig. 1). Two sites were selected to the study: the first one is Sharm El-Sheikh harbor, which is located at the entrance of the city as a small bay. It is located between latitudes (27° 50′ 46″ & 27° 51′ 24″ N) and longitudes (34° 16′ 32″ & 34° 16′ 45″ E). This bay is bounded on the northwest side of Gabal El-Safra (Fig. 2a) which consists of basement rocks and Miocene sedimentary rocks (Steckler et al. 1988; Sellwood and Netherwood 1984). Gabal El-Safra contains high concentrations of Fe, Mn, and Ni (Abu El-Enain and El-Sorogy 1994). In addition, some basement rocks also existed in the hinterlands which are scattered in many parts around the studied area. This bay is semi-circular in shape and occupies an approximate area of 1.4 km^2 with a narrow entrance to the sea in the southward by about 1000 m in width. This site is a tourist harbor of the city and it is always crowded with boats and yachts. The second site is Sharm El-Maya bay which is located to the east of the first site and located between latitudes (27° 51′ 21.13″ N & 27° 51′ 45.19″ N) and longitudes (34° 17′ 20.57″ E & 34° 17′ 54.42″ E). This bay is smaller than the first one by about 0.387 km^2. It is a semi-circular shaped bay and located away of Gabal El-Safra (Fig. 1). It seems closer than the other site by about 310 m to the entrance of the Gulf of Aqaba. It is surrounded by two headlands, Ras Umm-Sid in the northeast and the other in the southwest (Fig. 2b), which

separates Sharm El-Maya bay from the neighboring Sharm El-Sheikh harbor bay (Morsy et al. 2010).

Sampling sites were determined by GPS (Table 1). Samples were collected randomly using stainless-steel box sampler during winter 2019. They were transported to the laboratory into cloth bags in iceboxes. They were washed with distilled water and then left to dry in the room temperature. About 5 g of each sample was pulverized in an agate mortar for 15 min and sieved to 63 μm then dried in an oven at 80c. Two grams of this powder was digested in Teflon cups for 2 h in a mixture of (1 HF, 2 HClO$_4$, & 3 HNO$_3$). This solution was diluted with distilled water and was prepared for calculation. The atomic absorption spectrophotometer (AAS) was used to measure the heavy metal concentrations in the studied samples. The results were measured in micrometer. All standard precautions were taken when conducting the analyses and the accuracy of the analysis was verified by replicating the measurement of some samples.

Environmental statistical analysis

Some environmental factors and statistical analysis were used to evaluate the assessment of the extent of the environmental pollution of the study area and identify the expected sources responsible for the presence of pollutants in the environment such as metal pollution index (MPI), the contamination factor (CF), sediments pollution index (SPI), the geo-accumulation index (Igeo), ecological risk factor (ERI), the potential contamination index (Cp), and the enrichment factor (EF) according to their pollution indicators classification in Table 2. In addition to correlation coefficients, hierarchal cluster analysis (HCA) and principal component analysis (PCA) were calculated by using SPSS program.

Results and discussions

Special heavy metal distributions and worldwide comparison

The complete data analysis of the heavy metal concentrations was obtained in Table 1. Metal concentrations showed an irregular distribution pattern in the two studied sites. Sharm El-Sheikh harbor site contains different concentrations of metals ranged from the minimum to the maximum values as follows: Fe (1358–5467 μm);
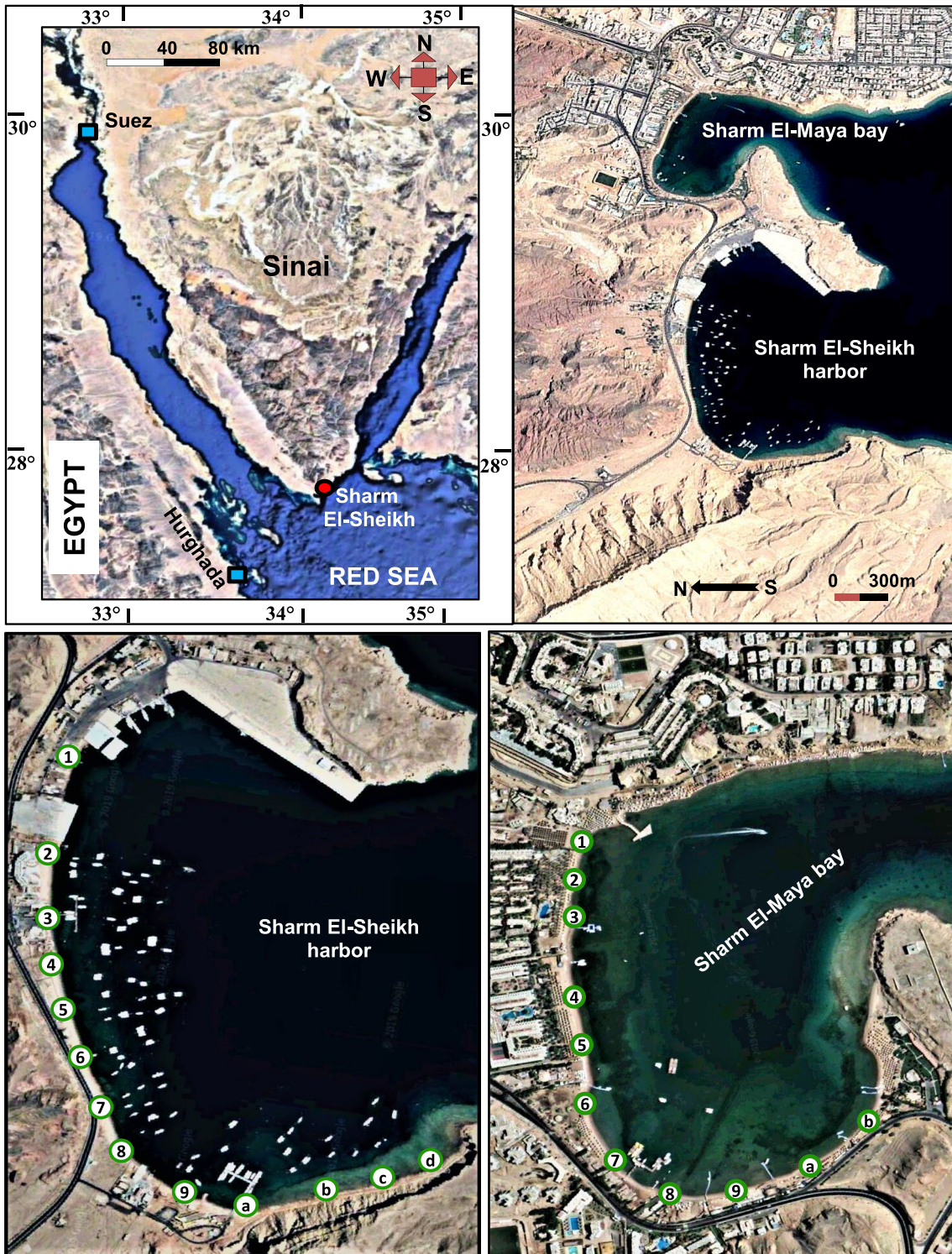
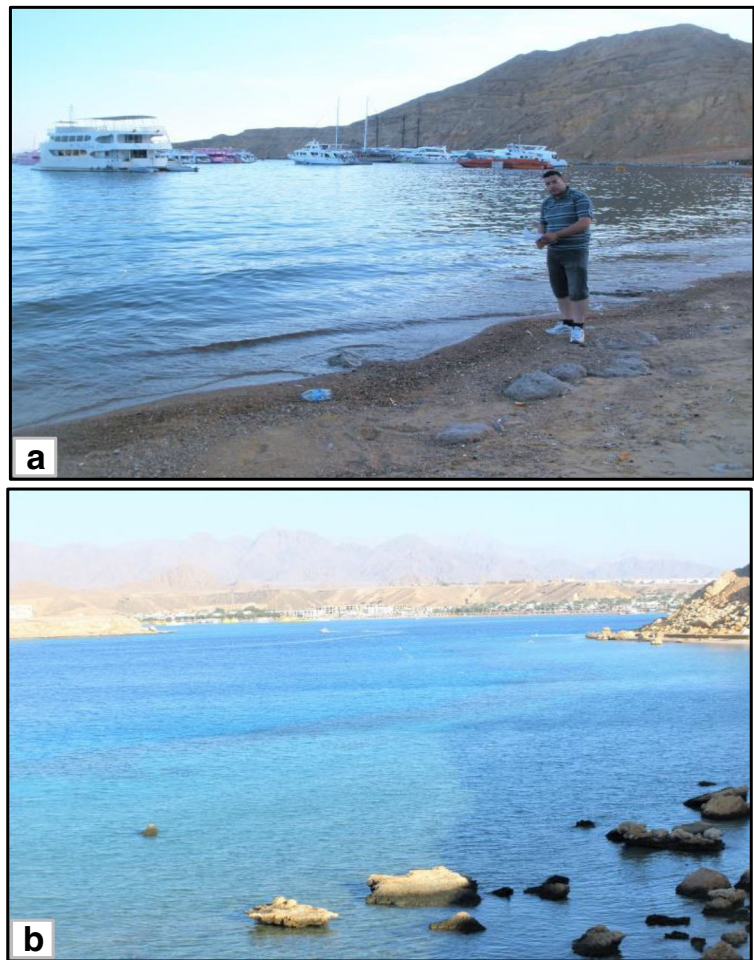**Note:** a= 10; b= 11; c= 12; d= 13

Fig. 1 Location map and sampling sites

Fig. 2 Close view of the study area

Mn (308–743 μm); Cu (17.25–39.21 μm); Zn (27.74–51.08 μm); Pb (22.14–42.15 μm); Ni (27.68–75.61 μm); Cd (1.78–3.12 μm); and Co (1.21–3.21 μm). On the other hand, Sharm El-Maya bay contains various heavy metal concentrations ranging from the minimum to the maximum values as follows: Fe (1223–3274 μm); Mn (158–564 μm); Cu (22.35–36.24 μm); Zn (29.24–48.24 μm); Pb (21.25–38.24 μm); Ni (20.68–64.25 μm); Cd (1.34–3.25 μm); and Co (0.89–3.11 μm).

The beach sediments of Sharm El-Sheikh harbor (Fig. 3) have a higher content of most of the studied heavy metals (Fe, Mn, Ni, and Cd) in comparison with Sharm El-Maya bay. These results are due to the fact that the Sharm El-Sheikh harbor is exposed to human pollutants represented by navigation movement of boats, plastics and wood rubbish, and fuel combustion products on the adjacent road which is very close to the shore (Fig. 4). In addition, metals transported by natural weathering of nearby mountain rocks (Gabal El-Safra) could be classified as potential sources as well. On the other hand, Sharm El-Maya bay is also affected mainly by human pollutants and decreased natural weathering effects as it is further away from Gabal El-Safra. At the same time, the presence of some basement rocks in certain places cannot be neglected. However, the differences in heavy metal concentrations in both bays are not very large and this may be attributed to the nature of each bay. Sharm El-Sheikh harbor is larger and connected to the sea by a wide entrance that may reach up to 1000 m in width, making water renewal much faster than Sharm El-Maya bay, where the later bay has an entrance of just 310 m, making the water movement more sluggish.

Figure 5 explains the comparison of the average concentrations of heavy metal distributions in the sediments of the two studied sites and other

Table 1 Heavy metal concentrations and metal pollution index values in studied sediments

Site	SN.	Lat.	Long.	Fe	Mn	Cu	Zn	Pb	Ni	Cd	Co	MPI
Sharm El-Sheikh harbor	H1	27° 51′ 26″	34° 17′ 04″	2447	421	29.47	38.31	34.12	27.68	2.67	1.21	37.05
	H2	27° 51′ 26″	34° 16′ 55″	4104	308	31.24	49.37	22.87	61.24	2.45	1.55	42.36
	H3	27° 51′ 25″	34° 16′ 46″	2057	664	30.25	43.21	37.24	33.24	2.77	1.34	41.02
	H4	27° 51′ 23″	34° 16′ 42″	1657	434	28.24	39.22	42.15	40.26	2.69	2.04	40.62
	H5	27° 51′ 23″	34° 16′ 40″	3019	388	33.51	51.08	36.25	55.47	2.78	1.87	46.26
	H6	27° 51′ 21″	34° 16′ 23″	1878	574	37.25	47.41	37.28	33.64	2.47	2.10	43.31
	H7	27° 51′ 17″	34° 16′ 28″	2578	367	39.21	42.37	35.69	72.24	2.99	3.21	49.97
	H8	27° 51′ 15″	34° 16′ 24″	2074	423	33.25	46.21	30.21	39.24	3.02	1.66	41.01
	H9	27° 51′ 08″	34° 16′ 20″	1358	441	29.21	38.11	22.14	58.54	1.78	1.47	35.02
	H10	27° 51′ 04″	34° 16′ 19″	5248	411	29.25	44.16	38.14	51.24	3.12	2.34	50.11
	H11	27° 50′ 59″	34° 16′ 21″	3015	420	27.45	27.74	33.25	33.78	2.57	1.55	37.96
	H12	27° 50′ 52″	34° 16′ 25″	5467	646	29.58	39.37	30.58	75.61	3.06	2.34	53.59
	H13	27° 50′ 48″	34° 16′ 29″	3157	743	17.25	44.11	33.24	53.58	3.11	1.89	45.59
Min.				1358	308	17.25	27.74	22.14	27.68	1.78	1.21	35.02
Max.				5467	743	39.21	51.08	42.15	75.61	3.12	3.21	53.59
Aver.				2928	480	30.40	42.36	33.32	48.9	2.73	1.89	43.37
Sharm El-Maya bay	M1	27° 51′ 41″	34° 17′ 48″	1845	322	26.47	39.21	27.12	59.24	1.66	1.22	34.49
	M2	27° 51′ 42″	34° 17′ 45″	2035	358	22.35	29.24	21.25	33.25	1.68	1.68	31.42
	M3	27° 51′ 43″	34° 17′ 42″	2147	367	31.24	41.25	32.58	26.25	2.66	2.64	39.64
	M4	27° 51′ 43″	34° 17′ 37″	2365	386	33.25	39.21	34.74	64.25	3.22	0.89	40.75
	M5	27° 51′ 43″	34° 17′ 33″	3274	501	29.24	37.12	38.24	36.24	3.25	1.47	43.04
	M6	27° 51′ 44″	34° 17′ 28″	3254	564	36.24	42.35	33.54	27.84	2.56	1.56	42.42
	M7	27° 51′ 43″	34° 17′ 24″	1223	398	27.14	44.62	37.25	30.24	1.34	1.48	32.73
	M8	27° 51′ 39″	34° 17′ 21″	1798	387	22.36	48.24	30.14	61.24	1.98	2.54	40.31
	M9	27° 51′ 36″	34° 17′ 22″	2179	364	32.58	43.25	27.54	20.68	2.47	2.87	38.18
	M10	27° 51′ 32″	34° 17′ 23″	2674	225	29.87	40.25	30.26	63.24	2.39	2.74	41.66
	M11	27° 51′ 28″	34° 17′ 25″	2254	158	33.25	47.25	32.58	21.24	2.14	3.11	35.59
Min.				1223	158	22.35	29.24	21.25	20.68	1.34	0.89	31.42
Max.				3274	564	36.24	48.24	38.24	64.25	3.25	3.11	43.04
Aver.				2277	366	29.45	41.09	31.385	40.34	2.30	2.02	38.20

worldwide localities. These results explained that the study area contains metal concentrations higher than those in other worldwide coasts, such as Fe, Mn, Cu, Zn, Ni, Cd, and Co of Hurghada (Nour et al. 2018); Mn, Cu, Pb, Ni, and Cd of Shalateen (Nour et al. 2019); Fe, Mn, Cu, Ni, and Cd of the Red Sea of Saudi Arabia (Youssef and El-Sorogy 2016); Cu, Zn, Pb, Ni, and Co of the Egyptian Mediterranean coast (Okbah et al. 2014); Fe, Mn, Cu, Zn, Pb, Ni, and Cd of the Libyan Mediterranean coast (Nour and El-Sorogy 2017); and Mn, Cu, Zn, Pb, Ni, and Cd of the Russian Caspian Sea (de Mora et al. 2004).

Assessment of sediment contamination

The results of the environmental indicators (Table 3) have been used to assess the heavy metal contaminations in the studied area. MPI values have been used to assess the degree of pollution and have been calculated according to Masoud et al. (2007) as MPI = $(C_1 \times C_2 \times C_3 \times C_n)^{1/n}$, where C is the concentration of metal in the sample and n is the number of metals. Metal pollution index (Table 1) showed that Sharm El-Sheikh harbor has a higher degree of pollution (43.4) than Sharm El-Maya bay (38.2). Samples H12, H10, and H7 have the highest MPI value (53.6, 50.1, and 49.97) respectively. This

Table 2 Classification of some environmental factors was used in the present work

Igeo	Forstner et al. (1993)	EF	Acevedo-Figueroa et al. (2006)
< 0	Unpolluted	< 1	No enrichment
0–1	Uncontaminated to moderately contaminate	1–3	Minor enrichment
1–2	Moderately polluted	3–5	Moderate enrichment
2–3	Moderately to strongly contaminated	5–10	Moderately severe enrichment
3–4	Heavily contaminated	10–25	Severe enrichment
4–5	Strongly to very strongly contaminated	25–50	Very severe
> 5	Extremely contaminated	> 50	Extremely severe
CF	**Hakanson (1980)**	**PERI**	**Qing et al. (2015)**
< 1	Low contamination	< 40	Low risk
1–3.	Moderate contamination	40–80	Moderate risk
3–6.	Considerable contamination	80–160	Considerable risk
> 6	Very high contamination	160–320	High risk
		≥ 320	Very high risk
Cp	**Davaulter and Rognerud (2001)**	**SPI**	**Chen et al. (2005)**
< 1	Low contamination	≤ 1	Low contamination
1–3	Moderate contamination	1–3	Moderate contamination
> 3	Severe or very severe contamination	> 3	High contamination

may be attributed to anthropogenic activities as heavy tourist activities, rubbish, navigation of boats' movements, and the nearby mountain hinterland. In addition, the natural weathering of Gabal El-Safra which contains high concentrations of Fe, Mn, and Ni (Abu El-Enain and El-Sorogy 1994). Lastly, the presence of many basement rocks scattered in the surrounding highlands can be described as a possible cause of such findings.

CF values were used to estimate the amplitude of metal contamination in sediments and calculated as CF $= C_m/C_b$ (Hakanson 1980), where C_m is the concentration of metals in the sample and C_b is the concentration of metals in the earth's crust. The results of CF (Table 3) illustrated that both of the studied sites are very high contamination with Cd (CF > 6) and moderately contaminated with Pb (CF = 1–3).

SPI values were used to identify single metal contamination indices and calculated as SPI = C_m/C_p (Kabata-Pendias and Pendias 2001), where C_m is the concentration of metals in the sample and C_p is the concentration of metals according to the permissible metal levels in sediments according to USEPA (1983). SPI results (Table 3) revealed that the both studied sites are highly contaminated with Cd, whereas Sharm El-Sheikh harbor was moderately contaminated with Cu,

Fig. 3 The comparison of heavy metal contents in sediments of both studied bays
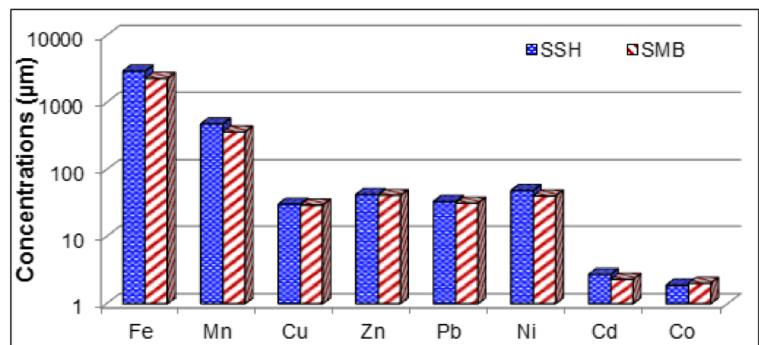
Fig. 4 Some human pollutants in Sharm El-sheikh harbor: **a** plastics and wood rubbish; **b** the navigation movement of boats; **c** fuel combustion products on the adjacent road
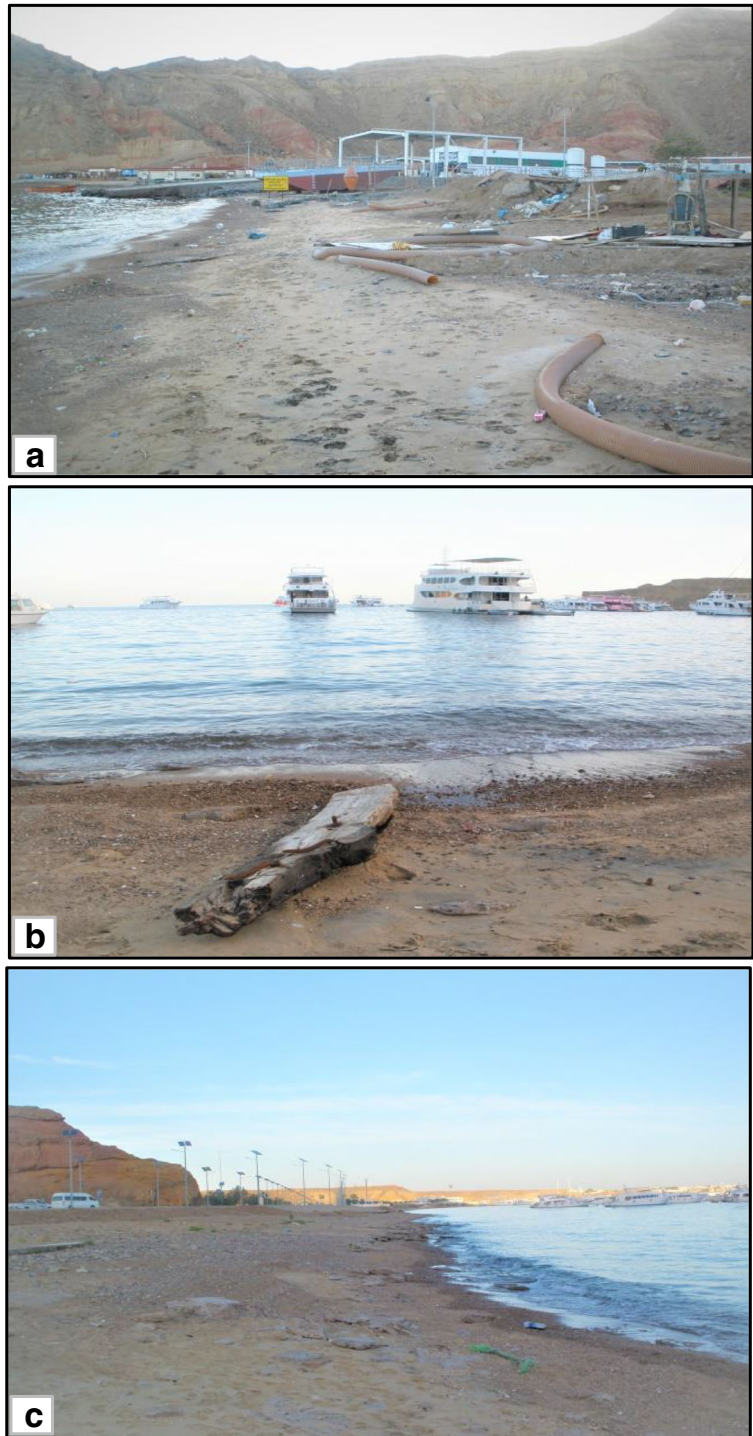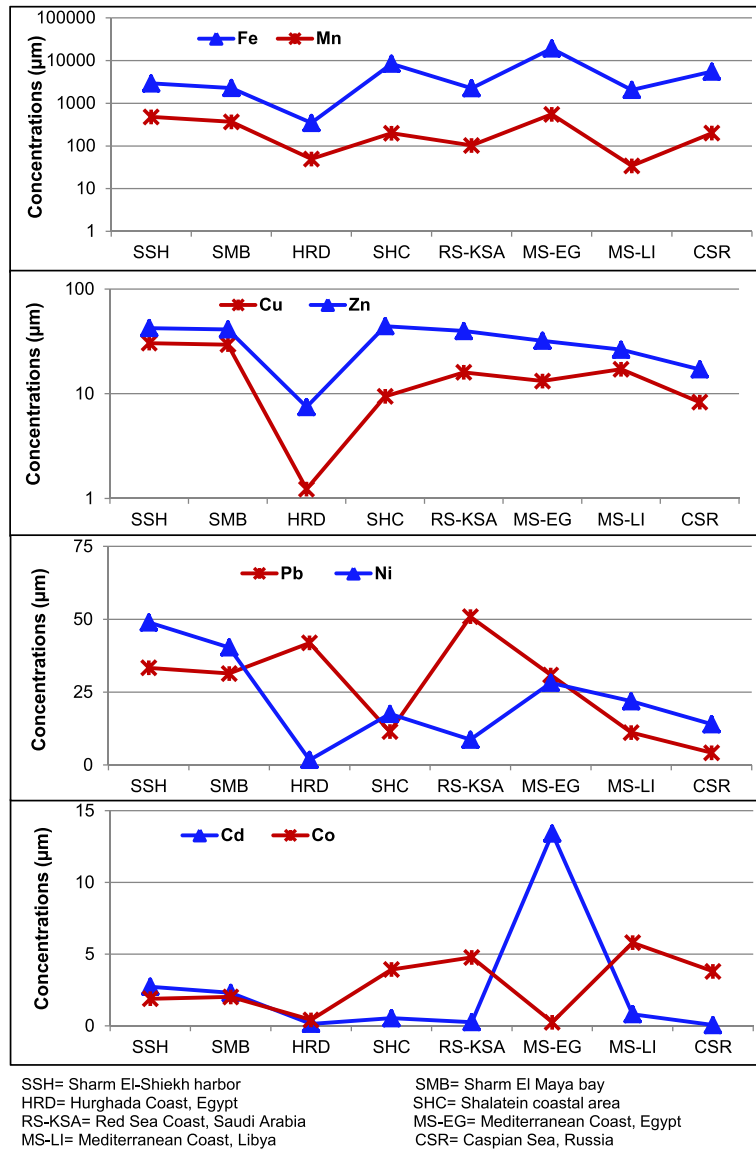

Pb, and Ni, and Sharm El-Maya bay was moderately contaminated with Pb and Ni.

Igeo values were used to determine the heavy metal pollution intensity in sediment and calculated as $I_{geo} = \log 2\ (C_m/1.5 \times M_b)$ according to Muller (1981), where C_m is the metal concentration in the sample and M_b is the metal concentration of shale (Turekian and Wedepoh 1961). I_{geo} values (Table 3)

Fig. 5 The comparison of the average heavy metal concentrations in the sediments of the studied area and other worldwide localities

SSH= Sharm El-Shiekh harbor   SMB= Sharm El Maya bay
HRD= Hurghada Coast, Egypt   SHC= Shalatein coastal area
RS-KSA= Red Sea Coast, Saudi Arabia   MS-EG= Mediterranean Coast, Egypt
MS-LI= Mediterranean Coast, Libya   CSR= Caspian Sea, Russia

showed that the both studied sites were moderate to strongly contaminated with Cd.

The ecological risk factor was used to assess the contamination of metals in sediments (Hakanson 1980) and calculated as $E^i_r = T^i_r \times C^i_f$, where T^i_r is a toxic response factor for metals according to Hakanson (1980) and C^i_f is the contamination factor of the metal. Therefore, the potential ecological risk index (PERI) can be calculated as the sum of E^i_r. These results demonstrated that the studied area is a highly contaminated risk with Cd where PERI value recorded (290 and 246) in Sharm El-Sheikh harbor and Sharm El-Maya bay respectively.

The potential contamination index (Cp) was calculated by the following method: $Cp = C_{max}/C_b$ (Hakanson 1980), where C_{max} is the maximum concentration of metal in the sample and C_b is the concentration of metal in the earth's crust (Turekian and Wedepoh 1961). Cp values clarified that Sharm El-Sheikh harbor and Sharm El-Maya bay were very severely contaminated with Cd and moderately contaminated with (Pb and Ni) in Sharm El-Sheikh harbor and (Pb) in Sharm El-Maya bay.

To evaluate the toxicity guidelines of heavy metals in the recent beach sediment of the studied area, the studied metal concentrations were compared with international

Table 3 The results of the environmental indicators in the studied area

Metals	CF			SPI			Igeo			PERI			EF			CP
	Min	Max.	Aver.	Min	Max.	Aver.	Min	Max.	Aver.	Min.	Max.	Aver.	Min.	Max.	Aver.	
							Sharm El-Sheikh harbor									
Fe	0.03	0.12	0.06				0.01	0.02	0.01							0.12
Mn	0.36	0.87	0.56	0.51	1.24	0.80	0.07	0.18	0.11				4.17	18.03	10.7	0.87
Cu	0.38	0.87	0.68	0.58	1.31	1.01	0.08	0.17	0.14	1.92	4.36	3.38	5.68	22.56	13.0	0.87
Zn	0.29	0.54	0.45	0.55	1.02	0.85	0.06	0.11	0.09	0.29	0.54	0.45	3.58	13.94	8.41	0.54
Pb	1.11	2.11	1.67	1.11	2.11	1.67	0.22	0.42	0.33	5.54	10.5	8.3	13.2	60.03	31.6	2.11
Ni	0.41	1.1	0.72	0.69	1.89	1.22	0.08	0.22	0.14	2.44	6.67	4.32	6.78	29.92	13.1	1.11
Cd	5.93	10.4	9.10	29.7	52.0	45.5	1.19	2.09	1.83	178	312	273	88.1	255.4	167	10.40
Co	0.06	0.17	0.10	0.15	0.40	0.24	0.01	0.03	0.02	0.32	0.84	0.50	0.94	3.093	1.84	0.17
							Sharm El-Maya bay									
Fe	0.03	0.07	0.05				0.01	0.01	0.01							0.07
Mn	0.19	0.66	0.43	0.263	0.94	0.61	0.04	0.13	0.09				3.89	18.07	18.07	0.66
Cu	0.50	0.81	0.65	0.745	1.21	0.98	0.10	0.16	0.13	2.48	4.03	3.273	9.37	23.28	23.28	0.81
Zn	0.31	0.51	0.43	0.585	0.96	0.82	0.06	0.10	0.09	0.31	0.51	0.433	5.63	18.13	18.13	0.51
Pb	1.06	1.91	1.57	1.063	1.91	1.57	0.21	0.38	0.31	5.31	9.56	7.846	24.3	71.88	71.88	1.91
Ni	0.30	0.94	0.59	0.517	1.61	1.01	0.06	0.19	0.12	1.82	5.67	3.559	5.94	23.64	23.64	0.94
Cd	4.47	10.83	7.68	22.33	54.2	38.4	0.90	2.17	1.54	134	325	230.5	124	214.2	214.2	10.83
Co	0.05	0.16	0.11	0.111	0.39	0.25	0.01	0.03	0.02	0.23	0.82	0.531	0.93	3.509	3.509	0.16

background values as well as with those in some regions around the world (Table 4 and Fig. 5). These results revealed that Cd content in the studied area is higher than its average concentration in the shale background (8.3 times), earth's crust (12.5 times), SQG (2.1 times), and ISQG (3.6 times). In spite of these results, Cd content in the study area is still under the probable effect level (PEL). Simultaneously, Pb and Ni metal contents in the study area showed higher concentrations than shale background, earth's crust, and ISQG, and SQG, ISQG, and PEL respectively.

Estimate the pollution sources

The enrichment factor was used to determine the potential source of pollutants, whether it is natural or anthropogenic. EF can be calculated as $(C_m/C_{Fe})/(C_{mb}/C_{bFe})$ according to Sinex and Helz (1981), where C_m is the concentration of metal in sample, C_{Fe} is the concentration of Fe in sample, C_{mb} is the concentration of metal in shale, and C_{bFe} is the concentration of Fe in shale (Turekian and Wedepoh 1961). EF values (Table 3) revealed that Sharm El-Sheikh harbor is extremely

Table 4 The comparison of the average metal concentrations in the studied area with international background values

Region	Fe	Mn	Cu	Zn	Pb	Ni	Cd	Co	Reference
Study area	2629	428	30	41.8	32.4	45	2.53	1.95	Present work
Background shale	47200	850	45	95	20	68	0.3	19	Turekian and Wedepoh (1961)
Background continental crust	56300	950	55	70	12.5	75	0.2	25	Taylor (1964)
Sediment quality guidelines	–	–	34	150	46.7	20.9	1.2	–	Long et al. (1995)
Interim sediment quality guidelines	–	–	18.7	124	30.2	15.9	0.7	–	ISQG (1995)
Probable effect levels	–	–	108	271	118	43	4.2	–	

Table 5 Heavy metal correlation coefficients in the studied area

	Fe	Mn	Cu	Zn	Pb	Ni	Cd	Co
Fe	1							
Mn	0.445*	1						
Cu	0.287	0.158	1					
Zn	0.271	0.257	0.506**	1				
Pb	0.288	0.482*	0.450*	0.402*	1			
Ni	0.503**	0.268	0.184	0.293	0.09	1		
Cd	0.640**	0.547**	0.465*	0.323	0.598**	0.361	1	
Co	0.324	0.023	0.423*	0.447*	0.287	0.202	0.275	1

*Correlation is significant at the 0.05 level (2-tailed)

**Correlation is significant at the 0.01 level (2-tailed)

enriched with Cd; very severely enriched with Pb; severely enriched with Mn, Cu, and Ni; and moderately severely enriched with Zn. On the other hand, Sharm El-Maya bay is extremely enriched with Cd and Pb, and severely enriched with Mn, Cu, Zn, and Ni. These results indicated that all studied metals were derived from anthropogenic sources where EF value > 1.5 according to Zhang and Liu (2002). The boat navigation, tourist activities, repainting boats, plastic wastes, and combustion of gasoline in motor vehicles are the possible sources of pollutants. In addition, wastewater may be one of the most important sources of certain metals such as Cd, Pb, and Co (Nour 2019).

The results of the correlation coefficient for the studied heavy metals (Table 5) illustrated that a strong positive correlation between Cd and each of Fe, Pb, and Mn ($r = 0.64$**, $r = 0.59$**, and $r = 0.55$** respectively) could be found. In addition, there is a good correlation between Cu and Zn ($r = 0.51$**) and Fe with Ni and Mn ($r = 0.5$** and 0.45*). The presence of this positive correlation between metals indicates that they may come from similar sources.

The results of dendrogram of hierarchal cluster analysis (HCA) and the principal component analysis (PCA) of heavy metals in the study area (Fig. 6 and Table 6) supported the results of the correlation matrix. The studied heavy metals divided into two clusters: cluster 1 consists of four sub-clusters (Fe-Cd, Mn, Pb, and Ni). While cluster 2 included two sub-clusters (Cu-Zn and Co). To emphasize that, PCA has arranged metals in three components with 72.973% of cumulative percentage: PC1 explains 43.616 % of the variance and clarified positive loading for Cd (0.821), Fe (0.723), Pb (0.695), Cu (0.662), Zn (0.654), Mn (0.614), Co (0.54), and Ni (0.524). PC2 demonstrated 15.8 % of the variance and showed positive loading for Co and Cu (0.591 and 0.45) respectively. Moreover, it shows negative loading for Mn, Fe, Cd, Ni, and Pb. PC3 revealed that 13.557 % of the variance and showed positive loading for Ni (0.697) and negative loading for Pb, Mn, Cu, and Cd. This result reveals that Cd, Fe, Pb, Cu, Zn, Mn, Co, and Ni may be derived from anthropogenic sources as boat navigation, repainting of boats, and the supply of fuel and tourist activities. Furthermore, the presence of Co, Ni, and Fe in

Fig. 6 The results of dendrogram of hierarchal cluster analysis in studied sediments
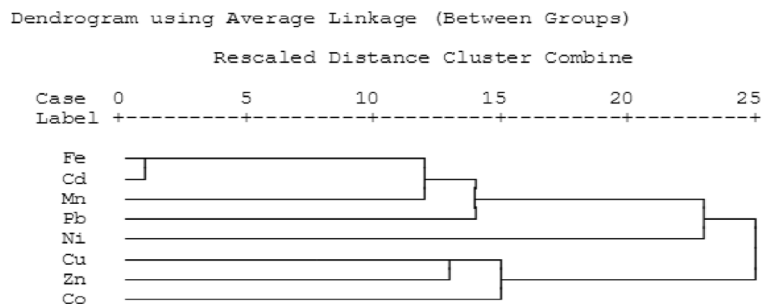
Table 6 Three principal component loadings for metals in the study area

Component matrix[a]

Metals	PC1	PC2	PC3
Fe	0.723	− 0.304	0.363
Mn	0.61	− 0.563	− 0.213
Cu	0.662	0.448	− 0.192
Zn	0.654	0.443	0.011
Pb	0.695	− 0.029	− 0.563
Ni	0.526	− 0.165	0.697
Cd	0.821	− 0.285	− 0.132
Co	0.54	0.591	0.224
% of variance	43.616	15.800	13.557
Cumulative (%)	43.616	59.416	72.973

[a] Three components extracted

PC2 and PC3 points to natural weathering especially from Gabal El-Safra and basement fragments.

Conclusions

The present study states that the sediments in the vicinity of the beach of Sharm El-Sheikh harbor contain concentrations of metals (Fe, Mn, Ni, and Cd) slightly higher than those in Sharm El-Maya bay. The environmental pollution indicators report that Sharm El-Sheikh harbor has a higher degree of pollution (MPI = 43.4) than Sharm El-Maya bay (MPI = 38.2). Both studied sites are very highly contaminated with Cd according to CF, Cp, EF, and SPI. The results of the ecological risk factor clarified that the studied area have a high risk of being contaminated with Cd where PERI value recorded (290 and 246) in Sharm El-Sheikh harbor and Sharm El-Maya bay respectively. In addition, they are moderately to highly contaminated with Pb, Mn, Cu, and Zn.

The studied area suffers from obvious human impacts due to heavy tourist activity, heavy boat navigation, large numbers of anchored tourist boats, the activity of vacationers, diving operations, and the car fuel combustion products on the main road which is very close to the beach. In addition, all these sources of natural pollution due to the weathering of the rocks of Gabal El-Safra and basement rocks play a role. However, the distribution of heavy metal concentrations in the both studied bays does not show significant differences between them, although Sharm El-Sheikh harbor is exposed to an increase in pollutants due to the natural weathering of the rocks of Gabal El-Safra that is rich in Fe, Mn, and Ni, which surrounds the bay by the West. This is mostly due to the nature and location of each of them, where Sharm El-Sheik harbor is characterized by a larger space and openness to the sea with a wide entrance up to 1000 m, while Sharm El-Maya bay has a smaller area and narrowing entrance to the sea by only 310 in width. The area of a given body of water and the breadth of the connection to the sea are important factors in speeding up water renewal process, wave movements, and the rates of sedimentation or erosion of the beach.

The present study shows that the studied area is enriched in Mn, Cu, Ni, and Cd of its counterparts in the Hurghada coast, the Shalateen coast, Red Sea of Saudi Arabia, and the Russian Caspian Sea. In addition, Cd, Pb, and Ni contents in the studied area are higher than its average in the shale background, earth's crust, SQG, and ISQG.

References

Abu El-Enain, F., El-Sorogy, A. (1994). *Microfacies, depositional environments and geochemistry of the Miocene carbonate succession of Gabal El Safra, southern Sinai, Egypt.* M.E.R.C. Earth Science Series Ain Shams Univ. 8, pp 167–177.

Acevedo-Figueroa, D., Jimenez, B., and Rodrigues-Sierra, C. (2006). Trace metals in sediments of tow estuarine lagoons from Puerto Rico. *Environmental Pollution,* 141, 336–342.

Chen, C., Kao, C., Chen, C., & Dong, C. (2007). Distribution and accumulation of heavy metals in the sediments of Kaohsiung harbour, Taiwan. *Chemosphere, 66,* 1431–1440.

Chen, T., Zheng, Y., Lei, M., Huang, Z., Wu, H., Chen, H., Fan, Ke-Ke. (2005). Assessment of heavy metal pollution in surface soils of urban parks in Beijing, China. *Chemosphere, 60,* 542–551.

Davaulter, V. and Rognerud, S. (2001). Heavy metal pollution in sediments of the Pasvik River drainage. *Chemosphere,* 42,9–18.

de Mora, S., Sheikholeslami, M., Wyse, E., Azemard, S., & Cassi, R. (2004). An assessment of metal contamination in coastal sediments of the Caspian Sea. *Marine Pollution Bulletin, 48,* 61–77.

Forstner, U., Ahlf, W., and Calmano, W. (1993). Sediment quality objectives and criteria development in Germany. *Water Science Technology, 28,*307.

Hakanson, L. (1980). An ecological risk index for aquatic pollution control. A sedimentological approach. *Water Research, 14,* 975–1001.

ISQG. (1995). *Interim Sediment Quality Guidelines* (p. 9). Ottawa: Environment Canada.

Kabata-Pendias, A., & Pendias, H. (2001). *Trace element in soils and plants* (4th ed.). London: CRC Press.

Long, E., MacDonald, D., Smith, S., & Calder, F. (1995). Incidence of adverse biological effects within ranges of chemical concentrations in marine and estuarine sediments. *Environmental Management, 19,* 18–97.

Masoud, M., EL-Samra, M., & EL-Sadawy, M. (2007). Heavy-metal distribution and risk assessment of sediment and fish from El-Mex Bay, Alexandria, Egypt. *Chemistry and Ecology, 23*(3), 201–216.

Morsy, M., Soliman, F., Khattab, R., Rashed, M., & El-Masry, N. (2010). Implications of environmental monitoring of oil pollution in Sharm El-Maya Bay, Sharm El-Sheikh, Egypt. *The Egyptian Society for environmental Sciences, 5*(1), 97–103.

Muller, G. (1981). Die Schwermetallbelastung der Sedimenten des Neckars und Seiner Nebenflusse. *Chemiker-Zeitung, 6,* 157–164.

Nour, H. E. (2019). Assessment of heavy metals contamination in surface sediments of Sabratha, Northwest Libya. *Arabian Journal of Geosciences, 12,* 177–186.

Nour, H. E., & El-Sorogy, A. (2017). Distribution and enrichment of heavy metals in Sabratha coastal sediments, Mediterranean Sea, Libya. *Journal of African Earth Science, 134*(273), 222–229.

Nour, H. E., El-Sorogy, A., Abdel-Wahab, M., Almadani, S., Alfaifi, H., & Youssef, M. (2018). Assessment of sediment quality using different pollution indicators and statistical analyses, Hurghada area, Red Sea coast, Egypt. *Marine Pollution Bulletin, 133,* 808–813.

Nour, H. E., El-Sorogy, A., Abd El-Wahab, M., Nouh, E., Mohamaden, M., & Al-Kahtany, K. (2019). Contamination and ecological risk assessment of heavy metals pollution from the Shalateen coastal sediments, Red Sea, Egypt. *Marine Pollution Bulletin, 144,* 167–172.

Okbah, M., Nasr, S., Soliman, N., & Khairy, M. (2014). Distribution and concentration status of trace metals in the Mediterranean coastal sediments, Egypt. *Soil and Sediment Contamination, International Journal, 23*(6), 656–676.

Qing, X., Yutong, Z., and Shenggao, L. (2015). Assessment of heavy metal pollution and human health risk in urban soils of steel industrial city (Anshan), Liaoning, Northeast China. *Ecotoxicology and environmintal safety,* 120,377–385.

Sellwood, B., & Netherwood, R. (1984). Facies evolution in the Gulf of Suez area: sedimentation history as an indication of rift initiation and development. *Modern Geology, 9,* 43–49.

Selvaraj, K., Mohan, V., & Szefer, P. (2004). Evaluation of metal contamination in coastal sediments of the Bay of Bengal, India: geochemical and statistical approaches. *Marine Pollution Bulletin, 49,* 174–185.

Sinex, S., & Helz, G. (1981). Regional geochemistry of trace elements in Checapeake Bay sediments. *Environmental Geology, 3,* 315–323.

Steckler, M., Berthelot, F., Lyberis, N., & Le Pichon, X. (1988). Subsidence in the Gulf of Suze: implications for rifting and plate kinematics. *Tectonophysics, 153,* 249–270.

Taylor, S. (1964). Abundance of chemical elements in the continental crust: a new table. *Geochimica et Cosmochimica Acta, 28,* 1273–1285.

Turekian, K., & Wedepoh, K. (1961). Distribution of the elements in some major units of the earth's crust. *American Geology Society Bulletin, 72,* 175–182.

USEPA (United States Environmental Protection Agency). (1983). Office of Solid Waste and Emergency Response. *Hazardous Waste Land Treatment, SW 874,* 273.

Wang, Q., Chen, Q., Yan, D., & Xin, S. (2018). Distribution, ecological risk, and source analysis of heavy metals in sediments of Taizihe River, China. *Environmental Earth Sciences, 77,* 569. https://doi.org/10.1007/s12665-018-7750-6.

Youssef, M., & El-Sorogy, A. (2016). Environmental assessment of heavy metal contamination in bottom sediments of Al-Kharrar lagoon, Rabigh, Red Sea, Saudi Arabia. *Arabian Journal of Geosciences, 9,* 474.

Zhang, J., & Liu, C. (2002). Riverine composition and estuarine geochemistry of particulate metals in China-weathering feature, anthropogenic impact and chemical fluxes. *Estuarine. Coastal and Shelf Science, 45,* 1051–1070.